Mechanism of Margination in Confined Flows of Blood and Other Multicomponent Suspensions

Amit Kumar and Michael D. Graham*

Department of Chemical and Biological Engineering, University of Wisconsin-Madison, Madison, Wisconsin 53706, USA
(Received 3 June 2012; published 4 September 2012)

Flowing blood displays a phenomenon called margination, in which leukocytes and platelets are preferentially found near blood vessel walls, while erythrocytes are depleted from these regions. Here margination is investigated using direct hydrodynamic simulations of a binary suspension of stiff (s) and floppy (f) capsules, as well as a stochastic model that incorporates the key particle transport mechanisms in suspensions—wall-induced hydrodynamic migration and shear-induced pair collisions. The stochastic model allows the relative importance of these two mechanisms to be directly evaluated and thereby indicates that margination, at least in the dilute case, is largely due to the differential dynamics of homogeneous (e.g. s-s) and heterogeneous (s-f) collisions.

Introduction.—Blood is a multicomponent suspension consisting primarily of red blood cells (RBCs) along with trace amounts of other components, primarily leukocytes and platelets [1,2]. Under physiological flow conditions, both the leukocytes and platelets segregate near the vessel walls [3], a phenomenon known as margination, while the RBCs tend to be depleted in the near-wall region forming a so-called "cell-free layer" [1,2]. Leukocytes are larger than RBCs and platelets smaller, but both are considerably stiffer than RBCs [4]; this difference is believed to play an important role in their margination. In addition, in illnesses such as malaria and sickle cell disease, the RBCs themselves are known to become stiff, and these stiffened cells also marginate [5]. Furthermore, delivery of drugs to tumors using particles injected into the bloodstream is a major goal of current cancer research [6]; margination may influence the distribution and thus the efficacy of these particles. Finally, there are many microfluidic applications where differences in the margination properties of various blood components are exploited to effect their separation [2,5,7].

Despite the importance of flow-induced segregation and margination phenomena in particle mixtures like blood, a mechanistic understanding is elusive [2]. The goals of the present work are to establish the mechanisms of rigidity-based margination in confined flows and to illustrate that these mechanisms are generic for multicomponent suspensions. We do this in two parts. First, we consider direct hydrodynamic simulations of a model problem that isolates the effect of stiffness on margination: a binary suspension of fluid-filled elastic capsules subjected to simple shear flow in a planar slit [8]. The two components of the binary mixtures have unequal membrane rigidities—the component with the higher rigidity is termed stiff, while the component with the lower rigidity is termed floppy. Additionally, we employ an idealized master equation (ME) model of the suspension dynamics that incorporates the two key transport mechanisms in confined suspensions:

(1) wall-induced particle migration and (2) particle displacements in homogeneous (e.g. stiff-stiff) and heterogeneous (stiff-floppy) pair collisions. We introduce a novel hydrodynamic Monte Carlo (HMC) simulation technique to find steady-state concentration distributions for this model. In contrast to direct numerical simulations, the ME-HMC approach allows the various aspects of the particle dynamics to be independently controlled, thereby enabling delineation of their role in the segregation behavior.

Using these approaches, we are able to isolate the effect of heterogeneous pair collisions and thus demonstrate their dominant role, at least in dilute systems, in the observed margination behavior. The approach and mechanisms presented here are generic for multicomponent suspensions—the model only takes as inputs the migration behavior of the various components of the suspension and their displacements upon homogeneous and heterogeneous collisions. Therefore, it is extensible to other systems including mixtures of particles of unequal sizes and shapes, thus encompassing whole blood flow as well as flow of drug delivery particles in the bloodstream.

Formulation.—We consider a suspension of fluid-filled neo-Hookean capsules [8] subjected to simple shear flow with shear rate $\dot{\gamma}$ between infinite parallel walls at $y = 0$ and $y = H$ [Fig. 1(a)]. At rest, all capsules are spheres with the same radius a. The rigidity of a particle is characterized by its membrane shear modulus G, which is expressed in terms of the nondimensional capillary number $\text{Ca} = \mu \dot{\gamma} a / G$, where μ is the viscosity of the suspending fluid. The capsules in a binary mixture with a lower $\text{Ca} = \text{Ca}_s$ are termed stiff, while the capsules with a higher $\text{Ca} = \text{Ca}_f$ are termed floppy; the number fraction of the floppy particles will be denoted X_f. The viscosity ratio λ of the fluid inside and outside the particle is unity. The Reynolds number is taken to be negligible.

In a dilute suspension of particles, particle interactions can be treated as a sequence of uncorrelated pair collisions
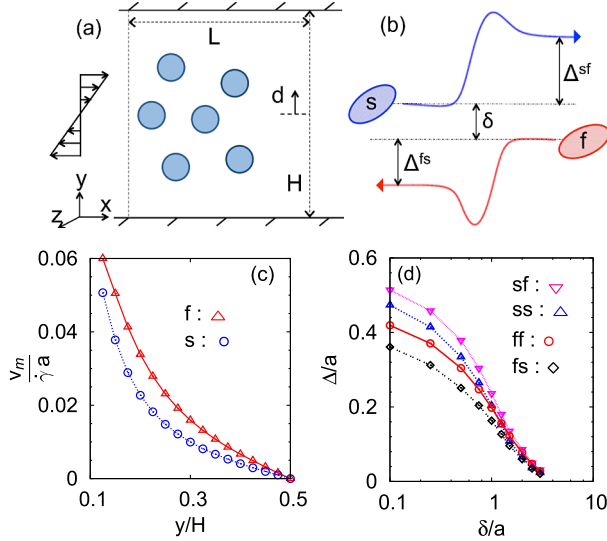
FIG. 1 (color online).   (a) System geometry, (b) schematic of
particle trajectories in a pair collision, (c) isolated particle
migration velocity at confinement ratio $2a/H = 0.197$, and
(d) cross-stream displacement Δ in various types of pair colli-
sions as a function of the initial offset δ. Here s refers to the
stiffer particle ($Ca_s = 0.2$), while f refers to the floppier particle
($Ca_f = 0.5$).

[9,10]. In addition, since the capsules are deformable, they
also have a wall-induced migration velocity $v_m(y)$ away
from the wall [11]. The effect of the pair collisions and the
wall-induced particle migration can be consistently
described by a kinetic master equation (cf. [9]). For sim-
plicity, we focus here on a model of a monolayer in the x-y
(flow-gradient) plane—extension to three dimensions is
straightforward [9]. The mean area number density of all
the particles in the monolayer is denoted n_0, such that the
areal fraction in the x-y plane at rest is $\phi_a = \pi a^2 n_0$.
The mean area number density of each of the species
α in the mixture is denoted n_0^α, while its distribution in
the y direction is denoted $n^\alpha(y)$. In this case, the master
equation is

$$\frac{\partial n^\alpha(y)}{\partial t} = -\frac{\partial (v_m^\alpha n^\alpha)}{\partial y} + \sum_{\beta=1}^{N_s} \bigg(\int_y^{y-H} [n^\alpha(y - \Delta^{\alpha\beta})$$
$$\times n^\beta(y - \Delta^{\alpha\beta} - \delta) - n^\alpha(y)n^\beta(y - \delta)]\dot{\gamma}|\delta| d\delta \bigg),$$
$$(1)$$

where δ is the precollision pair offset in the y direction,
$\Delta^{\alpha\beta}(\delta)$ is the cross-stream displacement of particle of type
α after collision with another particle of type β, while
the sum is over all the species N_s in the suspension; see
Fig. 1(b) for a schematic of a pair collision. The first term
on the right-hand side arises from the wall-induced migra-
tion, while the integral term represents the effect of pair
collisions [9].

This equation is analogous to the Boltzmann equation
for rarefied gases [12,13]. The dynamic simulation
Monte Carlo (DSMC) approach is a popular technique to
obtain solutions of the Boltzmann equation [12,13]. The
current work is inspired by the DSMC approach, which has
also found interest in recent works on colloidal suspensions
of rigid spheres [9]. By analogy, we term the method in the
present work as the hydrodynamic Monte Carlo (HMC)
method. As in the case of the DSMC technique [12,14], the
HMC approach is appropriate in the dilute limit and
requires the assumption of chaotic particle dynamics, an
assumption that is valid for the particulate flows considered
here [15].

In the HMC approach, the y positions of N_p particles are
followed in time. We set $N_p = 100$ here; simulations with
larger N_p gave indistinguishable results. Each particle is
assumed to represent an infinite number of particles at the
same y position randomly distributed in the flow direction
with an average spacing of L, where L is given by $L =
N_p/(n_0 H)$. A distinguishing feature of the HMC (or
DSMC) approach is that the collisions between particles
are treated probabilistically [14]. In the present study, we
neglect pair collisions with large initial offsets $\delta > \delta_{\text{cut}}$, as
their effect on cross-stream displacement is weak; we take
$\delta_{\text{cut}} = 2.5a$ here. A time step of the simulation involves
choosing a pair of particles which satisfies the condition
$\delta \leq \delta_{\text{cut}}$. The pair is subsequently selected or rejected for
collision with a probability proportional to the relative
velocity of approach of the two particles $\dot{\gamma}|\delta|$ [9,12,16].
An important aspect of the simulation is the time interval
between collisions Δt, because the wall-induced particle
migration occurs simultaneously with the collisions. In
order to determine Δt at each time step, we assume that
the number of particle collisions with time follows a
Poisson process with a mean collision frequency ν (ν is
estimated [17]), such that the time interval between colli-
sions is distributed with probability $P(\Delta t) = \nu e^{-\nu\Delta t}$ [16].
The distribution of time interval between collisions results
from the variation of particle positions in the flow direc-
tion, which is not explicitly specified. Once the collision
pair and time interval are set, we update positions of all
particles k as $y_k(t + \Delta t) = y_k(t) + v_m \Delta t + \Delta_k$, where Δ_k
is nonzero only for the colliding particle pair (i, j). If the
collision is homogeneous, then $\Delta_k = \Delta^{ss}$ or Δ^{ff} for stiff
and floppy particles, respectively. If the collision is hetero-
geneous, then $\Delta_k = \Delta^{sf}$ for the stiff particle and $\Delta_k = \Delta^{fs}$
for the floppy one. The procedure outlined above is
repeated until a statistical steady state is obtained. Other
details of the method can be found in Koura [16], whose
approach is closely followed here.

Pair collisions and wall-induced migration.—The HMC
method requires as inputs the cross-stream displacements
$\Delta^{\alpha\beta}$ in pair collisions and the wall-induced migra-
tion velocity v_m^α. These were computed using an acceler-
ated boundary integral method [8,18]; also see the

Supplemental Material [19]. Figure 1(c) shows the isolated particle migration velocity as a function of y/H for $Ca_s = 0.2$ and $Ca_f = 0.5$ capsules at a confinement ratio $2a/H = 0.197$. Results for $\Delta^{\alpha\beta}(\delta)$ for the same two species (in an unbounded domain) are shown in Fig. 1(d). For offsets $\delta \lesssim a$, $\Delta^{ff} < \Delta^{ss}$. Furthermore, an important feature in this plot, first reported in Ref. [8], is that the displacement of the stiffer particle in heterogeneous collisions is higher than that of the floppy particle ($\Delta^{sf} > \Delta^{fs}$), while the cross-stream displacements in homogeneous collisions are between these two limits, i.e., $\Delta^{fs} < \Delta^{ff}$, $\Delta^{ss} < \Delta^{sf}$. This ordering will turn out to be crucial in determining the segregation behavior.

The above particle migration velocity and pair collision results were determined in idealized systems, namely, by considering an isolated particle and an unconfined system, respectively. Our interest is in a *confined suspension*, so we expect that corrections will be necessary to both the migration and the pair collision results. For the migration velocity v_m, we note the wall-induced migration is due to the disturbance velocity created by the particle's image, and is a far-field effect [11]. As a result of its far-field nature, in a suspension of particles, it can be expected that the wall-induced migration of a particle will result not only due to interaction with its own images, but also due to images of other particles—this can be expected to introduce an averaging effect in a suspension of particle mixtures. To model this, we modify the migration velocities according to the following equation: $v_m^{\alpha,s} = \xi v_m^\alpha + (1 - \xi) \sum_1^{N_s} X_\beta v_m^\beta$, where $v_m^{\alpha,s}$ is the migration velocity of the species α in the suspension and ξ is an adjustable parameter. By taking $\xi = 1$, we recover the isolated particle migration velocity for each species, while for $\xi = 0$, each of the species in the suspension has the same migration velocity.

We adopt a similarly simple model to account for the confinement effects on the cross-stream displacement Δ in pair collisions. For a spherical particle with center at $y = a$, its Δ in a pair collision is expected to be zero as it will be touching the wall, while its Δ will approach the unconfined result at large particle-wall separations. To account for this effect, we multiply the Δ of the particle in an unconfined system by a factor $\eta = 1 - e^{-(d_w-a)/a}$, where d_w is the distance of the particle from the nearest wall, assumed to satisfy $d_w > a$. Despite this correction factor, particles might still occasionally overlap with the walls at high volume fractions, though that did not occur in the regime investigated here.

Validation.—We next validate the HMC method by comparing it with the results of detailed boundary integral (BI) simulations [8,18]. The suspensions in the BI simulations are fully three-dimensional, but otherwise are similar to those in the HMC method. The particle volume fraction in the BI simulations will be denoted ϕ_v. The HMC model has two adjustable parameters, n_0 (or ϕ_a) and ξ, which can

be tuned to obtain good agreement with BI simulations for a given suspension. In the present work, we seek the agreement of the mean normalized distance of a species from the centerline $\hat{d} = 2\bar{d}/H$ [see Fig. 1(a)] between the two methods.

The parameters n_0 and ξ in the HMC method are expected to depend on ϕ_v and $2a/H$, while their dependence on Ca_s, Ca_f, and X_f is expected to be weak. To demonstrate this, we focus on suspensions with $\phi_v = 0.04$ and $2a/H = 0.197$ held fixed. We then consider the BI results for a pure suspension with $Ca = 0.2$, and tune the value of n_0 in the HMC method to obtain a good match in $\hat{d}$ between the two methods; this yields $n_0 = 0.026a^{-2}$ (or $\phi_a = 0.082$). We next consider BI results for a binary mixture with $Ca_s = 0.2$, $Ca_f = 0.5$, and $X_f = 0.5$ and tune the value of ξ in the HMC method to obtain a good agreement in $\hat{d}$ of both the species between the two methods; this yields $\xi = 0.23$. Having set the value of n_0 and ξ, the HMC method can then be used to *predict* results for other suspensions at the same ϕ_v and $2a/H$. To establish this, we consider the same binary mixture as above ($Ca_s = 0.2$, $Ca_f = 0.5$) and predict $\hat{d}$ for both the species for a range of X_f and compare them with the corresponding BI results [Fig. 2(a)]. Excellent agreement can be observed at all values of X_f. Similar close agreement was also observed for different sets of (Ca_s, Ca_f), namely, (0.1, 0.5) and (0.3, 0.4) with no adjustment of n_0 and ξ (see the Supplemental Material [19]). Lastly, we consider a suspension with (Ca_s, Ca_f) of (0.2, 0.5) at $\phi_v = 0.12$ and $2a/H = 0.197$, and we tune the values of n_0 and ξ as discussed above, which yield $n_0 = 0.093a^{-2}$ (or $\phi_a = 0.292$) and $\xi = 0.63$. Subsequently, we predict $\hat{d}$ at various X_f in this system [Fig. 2(b)]. Excellent agreement is observed even at this higher volume fraction.

Besides the averaged measure $\hat{d}$, we also compared the particle number density distribution in the wall normal direction in the HMC and BI simulations. Results for the normalized number density distribution $\hat{n}_\alpha(y) = n_\alpha(y)/n_0^\alpha$ are shown in Figs. 2(c) and 2(d) for the $Ca_s = 0.2$ and
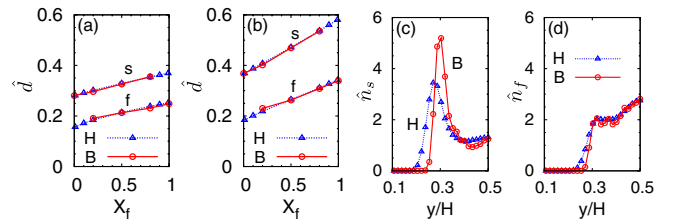

FIG. 2 (color online). (a),(b): Mean normalized distance of a species $\hat{d} = 2\bar{d}/H$ from the centerline in HMC (H) and BI (B) methods in (a) $(Ca_s, Ca_f, \phi_v) = (0.2, 0.5, 0.04)$ mixture as a function of X_f and in (b) (0.2,0.5,0.12) mixture. (c),(d): Normalized number density profile $\hat{n}$ for (c) stiff and (d) floppy particles at $X_f = 0.5$ for the suspension in (a). In all cases, $2a/H = 0.197$.

$Ca_f = 0.5$ mixture at $\phi_v = 0.04$, $2a/H = 0.197$, and $X_f = 0.5$; a more complete set of plots is provided in the Supplemental Material [19]. Very good agreement of $\hat{n}$ with the BI results is observed in all cases. The agreement is remarkably good in the region around the centerline, though the peak near the wall is usually smeared in the HMC results in comparison to the BI results. Nonetheless, given the broad agreement of $\hat{d}$ as well $\hat{n}$ in HMC and BI simulations in various suspensions, it is apparent that the HMC model captures the key aspects of the particle distributions in these suspensions.

Mechanisms of flow-induced segregation.—A key benefit of the HMC approach is that it allows independent investigation of the effect of various ingredients of the particle dynamics on the margination behavior. We focus here on suspensions with $Ca_s = 0.2$, $Ca_f = 0.5$, $\phi_v = 0.04$, and $2a/H = 0.197$. As discussed above, the HMC results for this system were generated by setting $n_0 = 0.026a^{-2}$ and $\xi = 0.23$. We first show the plots for $\hat{n}$ from the full HMC model for both the stiff and floppy particles at $X_f = 0.01$ (dilute in floppy) and $X_f = 0.99$ (dilute in stiff) in Figs. 3(a) and 3(d), respectively. It is clear from these plots that the *stiff* particles accumulate in the particle layer formed nearest to the wall as they become dilute in the suspension; i.e., they marginate with increasing X_f. In contrast, the *floppy* particles do the opposite as they become dilute (X_f decreases), accumulating near the centerline and thus "antimarginating." These trends agree

with the detailed boundary integral results of Ref. [8]; also see the Supplemental Material [19].

To disentangle the effects of wall-induced migration and pair collisions, we now consider a number of control cases. First, we investigate the impact of heterogeneous collisions, by (i) setting the particle migration velocities of both the species to the simple average migration velocity of these two species and (ii) setting Δ^{ss} and Δ^{ff} to the average value for the two species. Therefore, the only difference between these two species is their behavior in heterogeneous collisions: $\Delta^{sf} > \Delta^{fs}$. Plots of $\hat{n}(y)$ for these simulations are shown in Figs. 3(b) and 3(e). The difference between Δ^{sf} and Δ^{fs} is sufficient to lead to a segregation between the two species. In fact, as will be quantified shortly, most of the segregation results from heterogeneous collisions.

We next examine the effect of differences in migration velocity on the segregation behavior by setting the cross-stream displacement in all types of collisions for both the species to the simple average of the four curves on Fig. 1(d), yielding $\Delta^{sf} = \Delta^{ss} = \Delta^{fs} = \Delta^{ff}$. Plots for $\hat{n}(y)$ in this case are shown in Figs. 3(c) and 3(f). Here too some segregation is observed, though the degree of segregation is considerably smaller than in the full model.

The degree of segregation between the two species is more quantitatively characterized by computing the difference in $\hat{d}$ of each of the species from the corresponding pure species result; this is denoted by $\Delta\hat{d}$. The plots for $\Delta\hat{d}$ in various cases described above are shown in Figs. 4(a) and 4(b) for the stiff and floppy particles, respectively. For the present parameter set, the degree of segregation from the full model (case A) and the model where only heterogeneous collisions are distinct (case B) are almost identical, while that resulting from differences in the migration velocity (case C) is much weaker. In a recent direct simulation study [8], heterogeneous collisions were conjectured to play an important role in margination. In the simulations, however, it is not possible to deconvolve the effects of migration and collisions; i.e., one cannot perform control simulations. The ME-HMC approach does not suffer from this limitation.
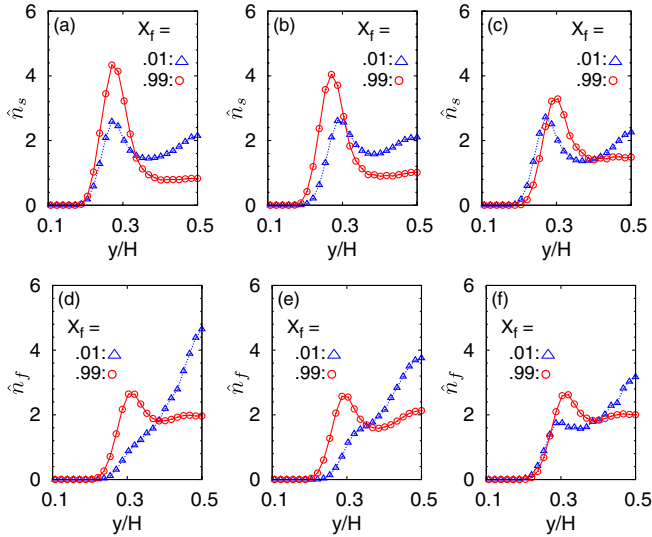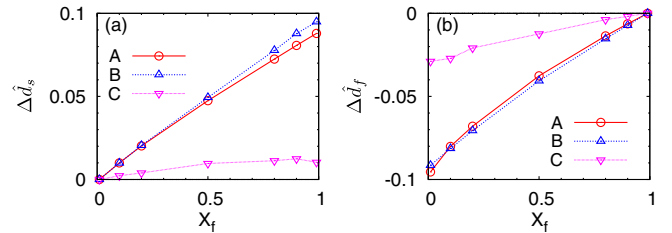

FIG. 3 (color online). Number density $\hat{n}$ for stiff (top row) and floppy (bottom row) particles in simulations at $X_f = 0.01$ and $X_f = 0.99$, from: (a),(d) full model (case A); (b),(e) only difference between the two species being heterogeneous collisions (case B); (c),(f) only difference between the two species being migration velocities (case C). These plots are for $(Ca_s, Ca_f, \phi_v) = (0.2, 0.5, 0.04)$.

FIG. 4 (color online). The difference $\Delta\hat{d}$ between $\hat{d}$ of a species in the mixture and the $\hat{d}$ of that species in its pure suspension for (a) stiff particles and (b) floppy particles in $(Ca_s, Ca_f, \phi_v) = (0.2, 0.5, 0.04)$ suspension. The cases A–C are described in the text.

Finally, we have investigated the effect of volume fraction on particle dynamics and margination. At $\phi_v = 0.12$, the effects of heterogeneous collisions and differential migration velocities (cases B and C) on margination become comparable (see the Supplemental Material [19]). Very similar results arise at $\phi_v = 0.2$ [19]. In the microcirculation, the volume fraction of cells is between $\phi_v = 0.1$–0.25 and it appears that, in this regime, both the migration velocity and the heterogeneous collisions are playing an important role in the segregation between the various species.

Conclusions.—To gain a mechanistic understanding of margination in blood and other multicomponent suspensions, we have introduced an idealized description of the particle flow dynamics that incorporates the two key transport mechanisms in confined suspensions: wall-induced migration and hydrodynamic pair collisions. The results for this model system clarify the important and previously underappreciated role played by heterogeneous collisions in the observed segregation behavior. Because differential behavior in heterogeneous collisions is generic for particles with contrasting shape or size as well as flexibility, the insights presented here are also applicable for other multicomponent suspensions. In particular, they have important implications in the design of drug delivery particles for optimal vascular wall targeting or for separating trace components of blood in microfluidic devices.

---

*graham@engr.wisc.edu

[1] A. S. Popel and P. C. Johnson, Annu. Rev. Fluid Mech. **37**, 43 (2005).

[2] A. Kumar and M. D. Graham, Soft Matter (to be published).

[3] G. J. Tangelder, H. C. Teirlinck, D. W. Slaaf, and R. S. Reneman, Am. J. Physiol., Heart Circ. Physiol. **248**, H318 (1985); J. C. Firrell and H. H. Lipowsky, *ibid.* **256**, H1667 (1989).

[4] J. B. Freund, Phys. Fluids **19**, 023301 (2007); H. Zhao and E. S. G. Shaqfeh, Phys. Rev. E **83**, 061924 (2011); D. A. Fedosov, J. Fornleitner, and G. Gompper, Phys. Rev. Lett. **108**, 028104 (2012).

[5] H. W. Hou, A. A. S. Bhagat, A. G. L. Chong, P. Mao, K. S. W. Tan, J. Han, and C. T. Lim, Lab Chip **10**, 2605 (2010).

[6] K. Loomis, K. McNeeley, and R. V. Bellamkonda, Soft Matter **7**, 839 (2011); H. Cabral, Y. Matsumoto, K. Mizuno, Q. Chen, M. Murakami, M. Kimura, Y. Terada, M. R. Kano, K. Miyazono, M. Uesaka *et al.*, Nature Nanotech. **6**, 815 (2011).

[7] S. S. Shevkoplyas, T. Yoshida, L. L. Munn, and M. W. Bitensky, Anal. Chem. **77**, 933 (2005).

[8] A. Kumar and M. D. Graham, Phys. Rev. E **84**, 066316 (2011).

[9] M. Zurita-Gotor, J. Blawzdziewicz, and E. Wajnryb, Phys. Rev. Lett. **108**, 068301 (2012).

[10] F. R. Da Cunha and E. J. Hinch, J. Fluid Mech. **309**, 211 (1996).

[11] J. R. Smart and D. T. Leighton, Phys. Fluids A **3**, 21 (1991); H. Ma and M. D. Graham, Phys. Fluids **17**, 083103 (2005).

[12] G. A. Bird, *Molecular Gas Dynamics and the Direct Simulation of Gas Flows* (Oxford University, New York, 1994).

[13] M. S. Ivanov and S. F. Gimelshein, Annu. Rev. Fluid Mech. **30**, 469 (1998).

[14] G. A. Bird, Annu. Rev. Fluid Mech. **10**, 11 (1978).

[15] G. Drazer, J. Koplik, B. Khusid, and A. Acrivos, J. Fluid Mech. **460**, 307 (2002).

[16] K. Koura, Phys. Fluids **29**, 3509 (1986).

[17] $\nu = 0.5 \int_0^L \int_0^H n(y)(\int_{y-\delta_{\text{cut}}}^{y+\delta_{\text{cut}}} n(y + \delta)\dot{\gamma}|\delta|d\delta)dy dx$.

[18] A. Kumar and M. D. Graham, J. Comput. Phys. **231**, 6682 (2012).

[19] See the Supplemental Material at http://link.aps.org/supplemental/10.1103/PhysRevLett.109.108102 for details on the calculation of pair collision and migration velocity results, comparison of the HMC and the BI results, and additional results on the effect of volume fraction on margination.